

PROGRESS OF PROFILE MEASUREMENT REFURBISHMENT ACTIVITIES AT HIPA

R. Dölling[†], E. Johansen, M. Roggli, M. Rohrer
Paul Scherrer Institut, 5232 Villigen PSI, Switzerland

Abstract

At PSI's High Intensity Proton Accelerator (HIPA) facility some 180 profile monitors and 10 radial probes are in use to measure transverse beam profiles in beam lines and cyclotrons at energies of 0.87 to 590 MeV. Mechanical malfunctions and increased noise in some devices, a lack of spare parts and the obsolescence of most of the driver and read-out electronics as well as extended requirements to the measurement, necessitate the development of improved versions of the electronics and of several monitors. We give an update on the status of three projects in this regard: A long radial probe in the Ring Cyclotron, a profile monitor and BPM at 590 MeV in high radiation environment and new loss monitor electronics, which should also serve as a basis for the profile monitor readout.

INTRODUCTION

Operation of HIPA started more than 40 years ago [1]. Meanwhile, a majority of HIPA beam diagnostics has reached an age of 20 to 35 years. Some twenty years ago, the focus of development resources shifted to PSI's newer accelerator facilities SLS, Proscan and SwissFEL. With the aging hardware, we have over the years, gravitated towards an increasingly critical situation. Many diagnostics need to be renewed or refurbished in the next decade.

Since HIPA is a user facility, accelerator development today proceeds at a much slower pace than in the initial years. Nevertheless, the approach based on Joho's N^{-3} scaling law [2, 3] is followed, where increased acceleration voltages in the RF cavities of the cyclotrons result in decreased beam losses and allow higher beam currents. A complementary approach [4, 5], based on a more detailed knowledge of beam and beam loss in the machine, would profit from profile measurements with high dynamic range or more than one dimension, as reported, e.g., in [6].

The replacement of components is a rare opportunity to adapt, improve or extend the functionality of diagnostics, which can support operation and development of the accelerator facility. At IBIC'19 and Cyclotrons'19 we reported on the start of the above mentioned three projects in this regard. For all three, we choose a design which allows later changes and improvements and already implements a number of concrete improvements. These projects will also generate expertise for the production of spares or the replacement of other similar monitors, respectively will serve as a basis for the replacement of the CAMAC profile monitor electronics. In the following, we give an update on the status and further steps of these projects.

[†] rudolf.doelling@psi.ch

RADIAL PROBE IN RING CYCLOTRON

We detailed the design of the basic version of the probe proposed in [7]. The downstream probe head will carry a vertical and two diagonal wires to determine the radial projected profiles of all turns and, to a certain degree [8], of most of the vertical profiles. Shielding electrodes at both sides along the probe carrier [7], which can be biased, will, hopefully, help to prevent disturbances by plasma clouds.

Realization of the hardware has progressed. The long service vacuum chamber including support, turbo pump and vacuum valves, as well as the mechanism to move the probe carrier into the cyclotron (Fig. 1) are ready. Fabrication of the rail guiding the carrier inside the cyclotron and of the 3-wire probe head (Fig. 2) is underway. The design of electrical feedthroughs and details of wiring nears completion. Wiring and lab testing of the complete assembly is still pending. We hope to be able to install the probe in the Ring Cyclotron in the coming, exceptionally short shutdown in February to replace the defect probe and to gain experience with the new design.

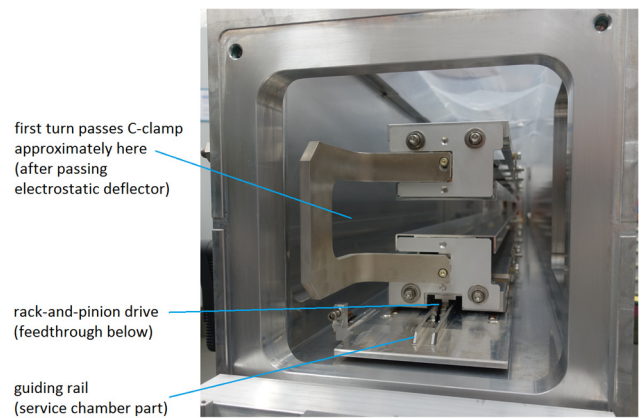


Figure 1: Probe carrier in parking position in the service chamber (in the lab, seen from cyclotron centre).

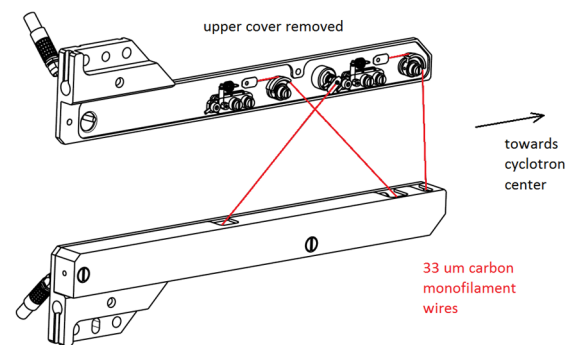


Figure 2: 3-wire probe head (seen from cyclotron side).

Content from this work may be used under the terms of the CC BY 3.0 licence (© 2020). Any distribution of this work must maintain attribution to the author(s), title of the work, publisher, and DOI

PROFILE MONITOR AND BPM IN SINQ BEAM LINE

We developed a detailed design for the monitor plug proposed in [9], which preserves the strict modularity (Figs. 3-6). To transfer the movement of the external drive to the profile monitor mechanism, we now intend to use a magnetic linear feedthrough from UHV Design Ltd. [10] (Fig. 5). NdFe magnets are used in the feedthrough and motor in order to achieve a lower activation than that with CoSm magnets. Alternatively, a conventional feedthrough with bellow can be used, requiring a much stronger motor. Force sensors measure the transferred force. This should allow an online diagnosis of the health of the mechanism at the highly activated lower end of the plug.

Procurement of components just starts. If production and assembly run smoothly, we may be able to install the plug, still without BPM, in the beam line in the coming shutdown to replace the defect monitor.

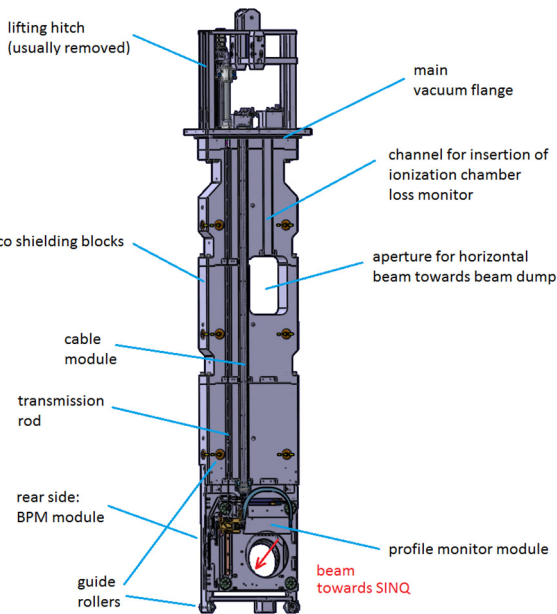


Figure 3: Monitor plug MHP45/46.

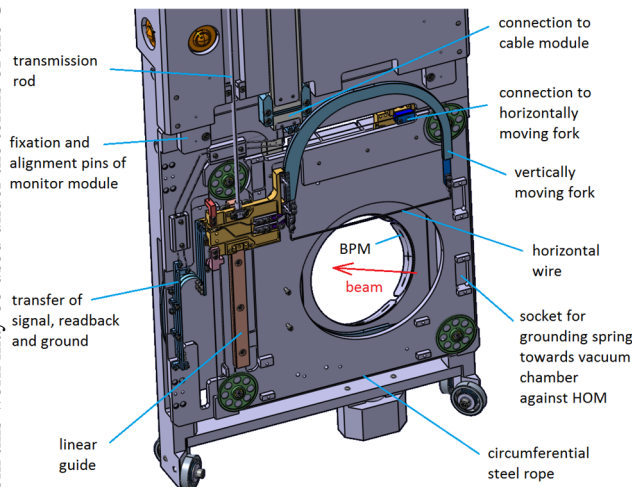


Figure 4: Profile monitor module.

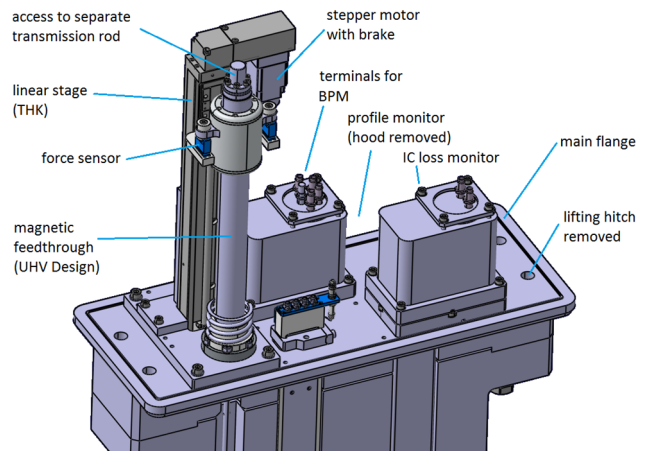


Figure 5: Upper part of monitor plug.

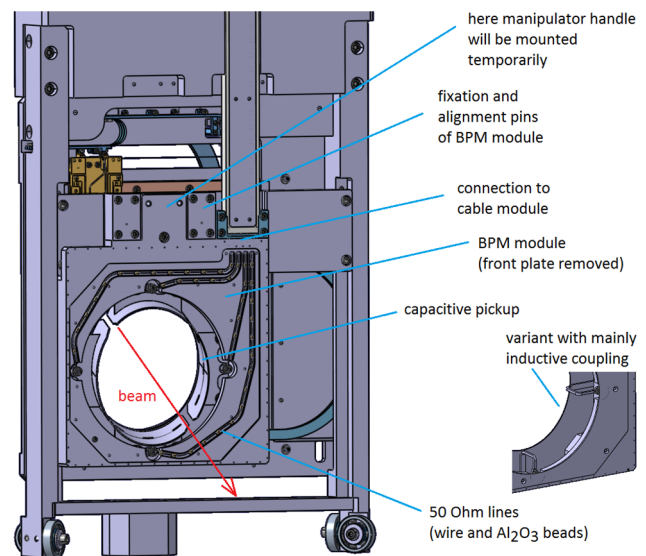


Figure 6: BPM module.

We plan to install, at the same time, a short version of this plug, without the three shielding blocks, together with a correspondingly shorter test chamber in the horizontal beam line towards UCN. There, radiation levels are much lower, and individual parts can be exchanged with hands-on access after testing. In particular, the BPM (Fig. 6), in a variant for horizontal beam, will be tested in order to evaluate the strength of higher order modes (HOM) and measures for their limitation. The situation should be comparable due to grounding springs between modules and towards the vacuum chamber located close to the BPM. Foregoing simulations are pending. Hence, manufacturing and installation of the BPM module will take place later.

The same design can be used at four plug locations, with only small variations to shielding blocks and BPM (horizontal/tilted/rectangular) or a double profile monitor unit for observation of both beam lines towards beam dump and SINQ. Dimensional changes are needed to accommodate the other six locations.

LOSS MONITOR ELECTRONICS

We improved the design of the electronics module discussed in [11] and studied the performed of the first prototype.

Log-Amplifier and Internal Shielding

The logarithmic transimpedance amplifier converts the measured current into a voltage. This circuit is very sensitive to noise and the circuit is under a metallic shielding. An ADL5304 from Analog Devices defines the core of the log-amplifier circuit. The bandwidth of the log-amplifier decreases at low input currents (Fig. 7).

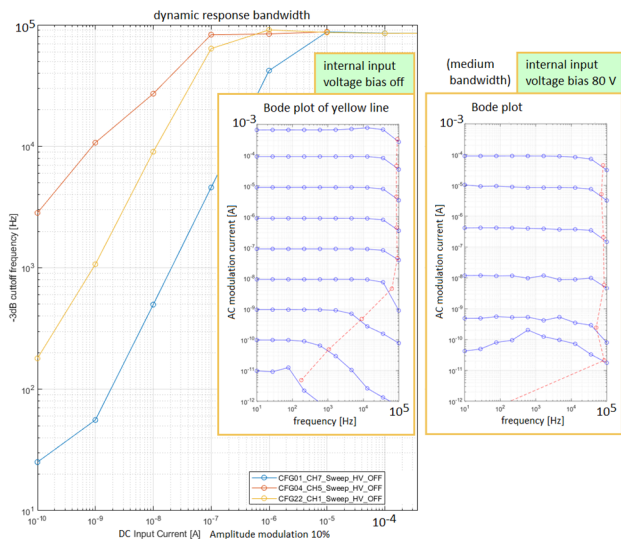


Figure 7: Bandwidth as function of input current for three circuit configurations. Without input voltage bias, the average of DC current is correctly represented within the bandwidth. With the bias on, this is the case only above a DC current of $\sim 30 \mu\text{A}$.

At higher currents above 10 nA the bandwidth is limited by the ADC anti-aliasing filter that is set to 50 kHz. With lower currents, the amplification in the log-amplifier is increased and the sensitivity to noise increases. A plot of a 10% current modulation is showing strong noise at a DC current of 1 nA (Fig. 8).

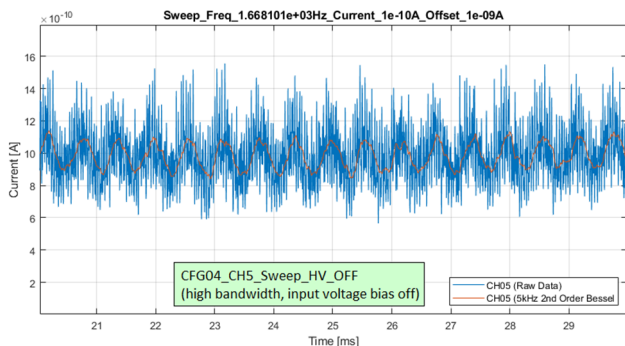


Figure 8: Measured current with 10% 1668 Hz modulation.

To find out where the noise comes from the amplitude spectrum was analysed (Fig. 9). Beside 50 Hz noise, there are several high-frequency spurs. To isolate the power supply of the log-amplifier, a Recom R1D-1205-R DC/DC

converter is used in the prototype. This circuit is switching typically at 60 kHz. The spectrum is showing that most noise stems from this DC/DC converter, as there is major peak in the spectrum at 60 kHz.

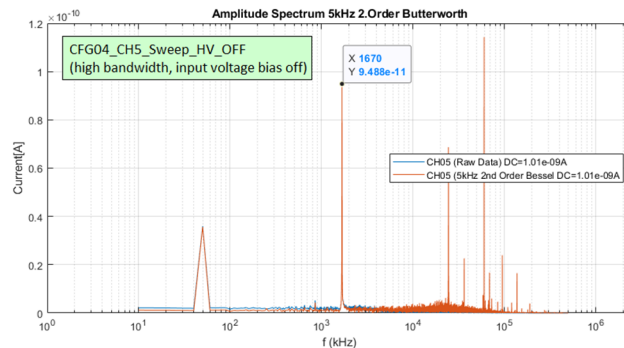


Figure 9: Amplitude spectrum from Fig. 8.

The actual layout provides no shielding between the DC/DC circuit and the log-amplifier because both are under the same shielding cover (Fig. 10). Switching noise from the DC/DC circuit couples strongly into the log-amplifier circuit.

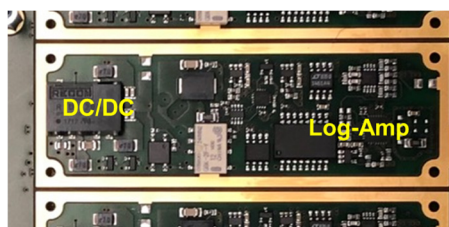


Figure 10: Layout of log-amplifier and DC/DC circuit.

The production circuit needs improvements to reduce the noise from the DC/DC converter. The following improvements are proposed: the DC/DC circuit is placed outside the log-amplifier shielding. The switching frequency of the DC/DC is increased.

The most important measure is to add shielding for the DC/DC converter noise. The shielding itself is more efficient at a higher frequency. Increasing the switching frequency also shifts the noise above the cut-off frequency of the anti-aliasing filter. This will contribute to less noisy signals seen by the ADC circuit.

In the prototype, the shielding material is aluminum, which has a low relative permeability and is not efficient for shielding low frequencies. It might therefore be a better choice to use standard shielding covers made out of cold rolled steel – CRS (Fig. 11). These shields have a resistivity of $4.6\text{e-}7 \Omega\text{m}$ and relative permeability of ~ 2000 . At a frequency of 60 kHz the skin depth in CRS is around 31 μm . This makes a 200 μm CRS shielding cover damping the field -56 dB at 60 kHz and -118 dB at 270 kHz – a higher switching frequency where commercial DC/DC converters are available.

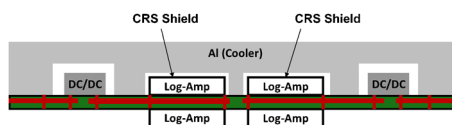


Figure 11: Improved shielding concept.

EMC

Electromagnetic compatibility is important to test and required to guarantee that the log-amplifier not goes into latch-up due to unexpected noise. Strong noise signals may occur due to lightning or switching of high-power equipment.

Fast transient bursts up to 500 V were applied to the signal cable utilizing a capacitive coupling clamp (Fig. 12). Higher levels were not tested at this time, because only two prototypes are available and there is potential risk of destroying the electronics at higher levels. The test criterion is IEC61000-4-4 type B: Measurement distorted, but the channel must recover to normal operation after the burst.

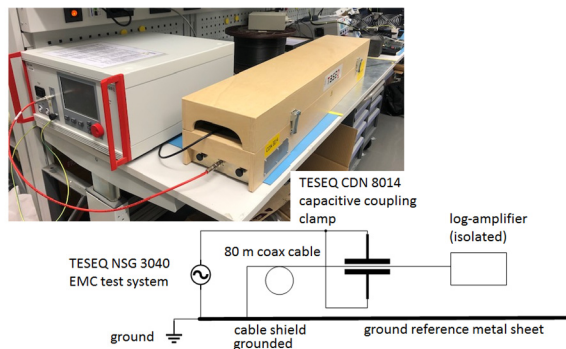


Figure 12: EMC burst test with capacitive coupling clamp.

Measurements of the output signal from the ADC is showing how the bursts influences the measured current strongly (Fig. 13). There is no latch-up and the circuit recovers after the bursts.

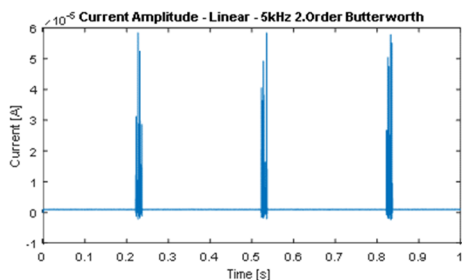


Figure 13: 1.0 μ A input current, -200V burst.

Moderate noise signals from external sources, as motor electronics or switching power supplies, coupled via cabling and ground, should not lead to a shift of the average signal level. Lab tests are foreseen to verify this.

Cooling

In the first prototype of the device, the focus was on circuit design. In the second prototype, the cooling design and manufacturability will take precedence. The first prototype showed that some components were not well cooled in the initial design. All components were operating inside the allowed temperature range, but for some components the temperature was quite high.

To improve the cooling and at the same time reduce the number of mechanical parts, a massive milled aluminium cooler replaces the cover plate of the device (Fig. 14). All

components with high power losses connect thermally directly to this cooler.

One component type with improved cooling are the SFP+ modules. These circuits are using improved cages with integrated thermal pad, called Thermal Bridge Technology [12]. The improved cooling lowers the temperature and increases expected lifetime for the electro-optical components.

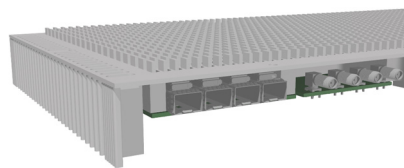


Figure 14: Improved cooling concept.

In addition, other components with high power consumption, like the System-on-Module and the 24 V DC/DC converter, connect with thermal pads directly to the cooler.

ACKNOWLEDGEMENTS

We like to thank Roger Senn for assembling the radial probe and contributing to its design. We thank Pedro Baumann, Gregor Gamma, Daniel Laube, Christian Nyfeler, Thomas Rauber, Roger Senn for providing information on the existing hardware, beam line environment and handling procedures, equipment and needs and for contributing to the mechanical design of the monitor plugs. We thank Roland Heyder for producing the CAD models and drawings for the monitor plugs. We thank Waldemar Koprek and Daniel Llorente for continued firmware support and Damir Anicic for Linux support.

AUTHOR CONTRIBUTIONS

MRog and EJ advanced the electronics. MRog performed the depicted measurements. RD advanced the monitor plug. MRoh advanced the long probe. EJ wrote the electronics chapter and RD the remaining parts of the paper.

REFERENCES

- [1] U. Schryber *et al.*, “Status report on the new injector at SIN”, in *Proc. Cyclotrons '81*, Caen, France, Sep. 1981, paper ABI-05, pp. 43-53.
- [2] W. Joho, “High intensity problems in cyclotrons”, in *Proc. Cyclotrons '81*, Caen, France, Sep. 1981, pp. 337-347.
- [3] C. Baumgarten, “Factors influencing the vortex effect in high-intensity cyclotrons”, in *Proc. Cyclotrons '19*, Cape Town, South Africa, Sep. 2019, pp. 270-274.
doi:10.18429/JACoW-Cyclotrons2019-WEB03
- [4] A. Adelman, R. Dölling, and M. Seidel, “Precise simulations of high-intensity cyclotrons”, PSI Scientific Report 2010, Villigen, Switzerland, pp. 54-55.
- [5] M. Frey, J. Snuverink, C. Baumgarten, and A. Adelman, “Matching of turn pattern measurements for cyclotrons using multiobjective optimization”, *Phys. Rev. Accel. Beams*, vol. 22, no. 6, p. 064602, 2019.
doi:10.1103/PhysRevAccelBeams

- [6] R. Dölling, “Bunch-shape measurements at PSI's high-power cyclotrons and proton beam lines”, in *Proc. Cyclotrons'13*, Vancouver, Canada, Sep. 2013, paper TU3PB01, pp. 257-261.
- [7] R. Dölling, G.G. Gamma, V. Ovinnikov, M. Rohrer, P. Rüttimeann, and R. Senn, “Development of a replacement for the long radial probe in the Ring Cyclotron”, in *Proc. Cyclotrons'19*, Cape Town, South Africa, Sep. 2019, pp. 86-89. doi:10.18429/JACoW-Cyclotrons2019-M0P024
- [8] L. Rezzonico *et al.*, “Diagnostics for high intensity beams”, in *Proc. BIW'94*, Vancouver, Canada, Oct. 1994, *AIP Conf. Proc.*, vol. 333, pp. 398-494, 1995.
- [9] R. Dölling *et al.*, “Development of modular spare parts for the profile and position monitors of the 590 MeV beam line at HIPA”, in *Proc. IBIC'19*, Malmö, Sweden, Sep. 2019, paper TUPP035, pp. 402. doi:10.18429/JACoW-IBIC2019-TUPP035
- [10] UHV Design Ltd, <http://www.uhvdesign.com>
- [11] R.Dölling, E. Johansen, W. Koprek, D. Llorente Sancho, and M. Roggli, “Development of new loss monitor electronics for the HIPA facility”, in *Proc. IBIC'19*, Malmö, Sweden, Sep. 2019, paper MOPP024, pp. 141. doi:10.18429/JACoW--MOPP024
- [12] TE connectivity, <https://www.te.com>